Fish and Shellfish Immunology 90 (2019) 40–51

Contents lists available at ScienceDirect

Fish and Shellfish Immunology

journal homepage: www.elsevier.com/locate/fsi

Full length article

Glutaredoxin 1 from big-belly seahorse (*Hippocampus abdominalis*): Molecular, transcriptional, and functional evidence in teleost immune responses

W.K.M. Omeka[1], D.S. Liyanage[1], Thanthrige Thiunuwan Priyathilaka, G.I. Godahewa, Seongdo Lee, Sukkyoung Lee[**], Jehee Lee[*]

Department of Marine Life Sciences & Fish Vaccine Research Center, Jeju National University, Jeju Self-Governing Province 63243, Republic of Korea

ARTICLE INFO

Keywords:
Disulfide reduction
Grx1
Hippocampus abdominalis
Immune responses
Redox homeostasis

ABSTRACT

Glutaredoxins (Grx) are redox enzymes conserved in viruses, eukaryotes, and prokaryotes. In this study, we characterized glutaredoxin 1 (HaGrx1) from big-belly seahorse, *Hippocampus abdominalis*. *In-silico* analysis showed that HaGrx1 contained the classical glutaredoxin 1 structure with a CSYC thioredoxin active site motif. According to multiple sequence alignment and phylogenetic reconstruction, HaGrx1 presented the highest homology to the Grx1 ortholog from *Hippocampus comes*. Transcriptional studies demonstrated the ubiquitous distribution of *HaGrx1* transcripts in all the seahorse tissues tested. Significant modulation ($p < 0.05$) of *HaGrx1* transcripts were observed in blood upon stimulation with pathogen-associated molecular patterns and live pathogens. The β-hydroxyethyl disulfide reduction assay confirmed the antioxidant activity of recombinant HaGrx1. Further, dehydroascorbate reduction and insulin disulfide reduction assays revealed the oxidoreductase activity of HaGrx1. HaGrx1 utilized 1,4-dithiothreitol, L-cysteine, 2-mercaptoethanol, and reduced L-glutathione as reducing agent with different dehydroascorbate reduction activity levels. Altogether, our results suggested a vital role of HaGrx1 in redox homeostasis as well as the host innate immune defense system.

1. Introduction

Glutaredoxins (Grxs) are known as glutathione-dependent thiol-disulfide oxidoreductases that are ubiquitously distributed in all living organisms [1]. They are small enzymes that belong to the thioredoxin superfamily but exhibit more versatile substrate activity than thioredoxins (Trxs) [2]. Grx family proteins have a number of isoforms with quite different structures and catalytic activities. They regulate essential and distinct biological functions in organisms.

Grxs can be classified into three categories based on their structure and catalytic properties. The first group is classical Grxs with a CXXC active site motif (usually CPYC) and a thioredoxin/glutaredoxin fold. Most vertebrate dithiol Grxs are included in this category. Members of the second category are structurally related to glutathione *S*-transferase but possess glutaredoxin oxidoreductase activity [3]. This category is characterized by a two-domain structure; the first domain contains a thioredoxin/glutaredoxin fold with CXXC and the second domain has an α-helical structure [2]. Grx2 from *E. coli* is representative of this category. The third category is defined as monothiol Grx which is represented by a monothiol active site (Normally CGFS) [4]. Grx3, Grx4, and Grx5 from *Saccharomyces cerevisiae* belong to this category [5]. Further, the human protein kinase C-interacting cousin of thioredoxin (PICOT) is considered a monothiol Grx that belongs to the third category [6].

Grxs are versatile oxidoreductases that reduce various substrates such as H_2O_2, ribonucleotide reductase, dehydroascorbate, arsenate reductase, and others [3,4]. The typical Grx catalytic mechanism is similar to that of Trxs, which catalyze thiol-disulfide exchange using the CXXC motif, but Grx depends on GSH as an electron donor [7]. Many of the substrates utilized by Grxs are essential to DNA synthesis, collagen synthesis, and maintain redox homeostasis [4]. Further, Grxs have been identified as a universal iron-sulfur cluster (Fe/S-cluster) coordinating proteins [7]. Fe/S-clusters are inorganic cofactors that facilitate electron transfer reactions, redox reactions, and protein folding [1].

[*] Corresponding author. Marine Molecular Genetics Lab, Department of Marine Life Sciences, College of Ocean Science, Jeju National University, 66 Jejudaehakno, Ara-Dong, Jeju, 690-756, Republic of Korea. .

[**] Corresponding author.

E-mail addresses: lskshiny@hotmail.com (S. Lee), jehee@jejunu.ac.kr (J. Lee).

[1] These authors contributed equally to this work.

https://doi.org/10.1016/j.fsi.2019.03.078
Received 27 November 2018; Received in revised form 2 March 2019; Accepted 30 March 2019
Available online 20 April 2019

Regarding immunity, Grxs play a vital role in both viruses and humans. For example, Phage T4, *Vaccinia, Ectromelia,* and smallpox viruses produce their own Grx that is essential for DNA synthesis, disulfide bond formation, and virus assembly [2,8,9]. Additionally, human Grx1 regulates the activity of HIV-1 protease activity and thus is vital for regulating protease activity in HIV-1-infected cells [10]. Moreover, Grxs demonstrated a crucial role in defending cardiomyocytes from oxidative stress by regulating the NF-κB pathway [11]. In lung epithelial cells, Grx1 acts against bacterial infections by promoting *S*-glutathionylation of NF-κB family proteins [12]. Further, Grxs play an essential role in the nervous system and reproduction system in mammals [13–16].

Grx activity has been highly studied in eukaryotes [17], prokaryotes [18], and viruses [8]. For example, Grxs from mammals and *E.coli* have been studied for their oxidoreductase activity [17,19,20] and thiyl radical scavenging and transferase properties of human Grx have been examined [21]. However, there are few reports about Grx activity related to fish immunity and redox homeostasis. Only Grx2 from zebrafish was investigated for its role in Fe/S cluster coordination, brain development, and heart development [1,22,23]. Moreover, transcriptional modulation of Grx1 and Grx2 from Manila clam were reported [24]. However, there have been no functional studies on Grx1 in teleosts to date.

Seahorses are a group of aquatic animals that have exploited for years for their medicinal and ornamental properties. Annually, around 20 million seahorses are collected from the wild for medicinal purposes alone [25]. Therefore, seahorses have been included in global conservation programs (CITES) and cultivated for commercial use by many countries including Australia and Indonesia [25,26]. Big-belly seahorse (*Hippocampus abdominalis*) is the largest seahorse species and is naturally distributed in the Korean peninsula and around the ocean [19]. Being a large, smooth-skinned species provides a high market value for big-belly seahorses. However, fulfilling the demand for seahorses is still a problem as they are extremely difficult to culture. One of the major threats for seahorse cultivation is their poor adaptability to higher densities and stressful environments, thus increasing their vulnerability to pathogenic infections [27]. Therefore, understanding the immune responses of big-belly seahorse against bacterial and pathogen-associated molecular pattern (PAMP) stimuli will facilitate the development and maintenance in seahorse cultivation. Accordingly, the present study investigated the molecular, transcriptional, and functional properties of Grx1 from big-belly seahorse (HaGrx1) to understand its role in immunity.

2. Materials and methods

2.1. Identification of Grx1 from H. abdominalis

The cDNA sequence with the highest homology to Grx1 was obtained from the big-belly seahorse transcriptomic database which was established previously [28]. National Center for Biotechnology Information (NCBI) BLAST algorithm and RefSeq non-redundant protein databases were used to compare and verify the obtained sequence [29].

2.2. Bioinformatic analysis of HaGrx1 sequences

The coding sequence of HaGrx1 was obtained using the NCBI ORF Finder (https://www.ncbi.nlm.nih.gov/orffinder/) and putative polypeptide sequence was derived. Then, the amino acid sequence was verified using the NCBI blastp program [30]. ExPASy Protparam [31] was used to study the physiochemical properties of the HaGrx1 protein and predicted N-linked glycosylation sites were recognized by NetNGlyc 1.0 server [32]. Further, signal peptides of HaGrx1 were analyzed by the SignalP 4.1 online tool [33]. The domain organization and signature motifs in the HaGrx1 amino acid sequence were analyzed by the NCBI conserved domain database [34] and Motif Scan [35]. The SWISS model workbench [36] was used to predict the tertiary structure of HaGrx1 by comparison with the crystal structure of human glutaredoxin 1 in its fully reduced form as a template (PDB; jhb.1). The predicted three-dimensional structure of the HaGrx1 protein was pictured by using PyMOL software. Multiple sequence and pair-wise sequence alignments were generated by Clustal Omega [37] and EMBOSS needle tools [38], respectively. The phylogenetic tree was constructed using the neighbor-joining method available in MEGA7 software with 5000 bootstraps to investigate the relationship between HaGrx1 with other Grx1 orthologs [39].

2.3. Sample collection for tissue-specific distribution and temporal expression analysis

Sample collection for both tissue distribution and the temporal expression was carried out as described previously [28]. Healthy big-belly seahorses were acquired from the Korea Marine Ornamental Fish Breeding Center (Jeju Island, Republic of Korea) and kept in 300 L tanks with temperature of 18 ± 2 °C and practical salinity units (psu) of 34 ± 0.6 for a one-week period. Then, six healthy big-belly seahorses (three males and three females with an average body weight of 8 g) were dissected and 14 tissues including liver, testis, ovary, spleen, intestine, gill, kidney, skin, muscle, heart, pouch, stomach and brain were carefully isolated for tissue-specific transcriptional analysis. Blood was collected by tail cutting and the peripheral blood cells were separated by centrifugation at 3000 × *g* for 10 min at 4 °C. Then, all tissues were immediately snap frozen in liquid nitrogen and stored at −80 °C.

For the temporal expression analysis experiment, big-belly seahorses were divided into five groups, and each group contained 35 juvenile big-belly seahorses having an average body weight of 3 g. Each group was intraperitoneally injected with 100 μL of lipopolysaccharides (LPS) (1.25 μg/μL), polyinosinic:polycytidylic acid (poly I:C) (1.5 μg/μL), *Edwardsiella tarda* (5×10^3 CFU/μL), and *Streptococcus iniae* (1×10^5 CFU/μL), which were suspended phosphate buffered saline (PBS). The control group was injected with 100 μL of PBS. Next, blood was collected from five seahorses at 3, 6, 12, 24, 48, and 72 h post-injection (p.i.) intervals. During the temporal expression analysis experiment period, seahorses were not fed. All experiments in this study including seahorse rearing and temporal expression were reviewed and approved by the Animal Care and Use Committee of Jeju National University.

2.4. RNA extraction and cDNA synthesis

Total RNA was extracted from a pool of excised tissues (tissue distribution n = 6 and temporal expression n = 5) using RNAiso plus reagent (TaKaRa, Japan) and cleaned up with RNeasy spin column (Qiagen, USA) according to the manufacturer's protocol. The quality of the extracted RNA was assessed by 1.5% agarose gel, and the concentration was recorded at 260 nm using a μDrop Plate (Thermo Scientific, USA). Then, 2.5 μg of total RNA was reverse transcribed using the PrimeScript™ II 1st Strand cDNA synthesis kit (TaKaRa, Japan). Finally, synthesized cDNA was diluted 40-fold in nuclease-free water and stored at −80 °C.

2.5. Quantitative real-time PCR (qPCR) analysis

Tissue-specific and temporal mRNA expression of *HaGrx1* was measured by qPCR using TaKaRa Thermal Cycler Dice Real Time System III. All qPCR primers were designed according to the minimum information for publication of quantitative real-time PCR experiments (MIQE) guidelines [40] using the IDT primer quest tool (https://sg.idtdna.com). Big-belly seahorse 40S ribosomal protein S7 gene (Accession No: KP780177) was selected as an internal control gene. The qPCR reaction was performed in a total 10 μL reaction mixture composed of 3 μL of cDNA template, 5 μL of TaKaRa Ex Taq™ SYBR premix

(TaKaRa, Japan), 1.2 μL of PCR grade water, and 0.4 μL of each primer (10 pmol/μL) as cited in Table 1. Initial denaturation, denaturation, annealing, and extension parameters for a qPCR cycle were 10 s at 95 °C, 5 s at 95 °C, 10 s at 58 °C, and 20 s at 72 °C, respectively. After 45 cycles, a final cycle of 15 s at 95 °C, 30 s at 60 °C, and 15 s at 95 °C was run to evaluate the specificity of target amplification.

2.6. Statistical analyses of qPCR data

Relative mRNA expression of *HaGrx1* was calculated by the Livak ($2^{-\Delta\Delta CT}$) method [41]. For tissue-specific expression data analysis, the Ct value of skin tissue was set as the basal expression. Relative *HaGrx1* expression values were statistically analyzed by one-way ANOVA using IBM SPSS 24 software (SPSS, USA). For the immune challenge expression analysis, mRNA expressions at different p.i. intervals were represented as fold changes relative to the PBS and unchallenged controls at each time point. Fold values were further statistically compared ($p < 0.05$) with un-injected control (0 p.i) by the Mann-Whitney *U* test using the IBM SPSS 24 software. All determinations were carried out in triplicates and the results are expressed as the mean ± standard deviation (SD).

2.7. Recombinant plasmid construction

Specific cloning primers with corresponding restrictions sites were designed for recombinant plasmid construction (Table 1). The HaGrx1 coding sequence was amplified by PCR using template cDNA derived from blood. The total volume of 50 μL of PCR reaction mixture was prepared by adding 0.4 μL of Ex Taq polymerase (5 U/μL, TaKaRa, Japan), 2 μL (10 pmol/μL) of respective forward and reverse primers, 5 μL of 10 × ExTaq buffer, 4 μL of 2.5 mM dNTP, and 10 μL of 40-fold diluted cDNA. The PCR conditions were as follows: an initial denaturation at 94 °C for 4 min, followed by 35 cycles at 94 °C for 30 s, 56 °C for 30 s, 72 °C for 70 s, and a final extension at 72 °C for 10 min. Then, the PCR product was purified by the Accuprep® PCR purification kit (Bioneer Co., Korea). Amplified PCR products and the pMAL c5x vectors (New England BioLabs Inc.) were subjected to restriction digestion with respective restriction enzymes according to the manufacturer's instructions (TaKaRa, Japan). Next, PCR fragments and the pMAL c5x vectors were subjected to gel electrophoresis and purified by the Accuprep® Gel purification kit (Bioneer Co., Korea). Digested pMAL c5x vector and HaGrx1 fragments were ligated by Ligation Mighty Mix (TaKaRa, Japan) for 30 min at 16 °C. Then, recombinant vectors were transformed into *Escherichia coli* (DH5α) competent cells by the heat-shock method and positive clones were isolated by the Accuprep® Plasmid Mini Extraction kit (Bioneer Co., Korea). Finally, the sequence of recombinant HaGrx1 (rHaGrx1) was confirmed by sequencing (Macrogen, Korea).

2.8. Overexpression and purification of HaGrx1 fusion protein

The recombinant plasmids with verified sequences were transformed into *E. coli* BL21 (DE3) competent cells and cultured in Luria-Bertani (LB) rich ampicillin medium (LB + 0.2% glucose, 100 μg/mL of ampicillin). Cells were incubated at 37 °C at 200 rpm until growth reached an optical density at 600 nm (OD_{600}) of 0.5. Then, rHaGrx1 protein expression was induced by adding 1 mM isopropyl β-D-1-thio-galactopyranoside (IPTG) solution and further incubated at 25 °C and 200 rpm for 8 h. At the end of the incubation process, cells were harvested by centrifugation at 3000 × *g* for 30 min at 4 °C. The pellet was resuspended in 25 mL column buffer (20 mM Tris-HCl pH 7.4 and 200 mM NaCl) and stored at −20 °C for overnight. Cold resuspensions were thawed and lysed by cold sonication. Then, rHaGrx1 protein was purified as a fusion protein of maltose binding protein (MBP) by pMAL protein fusion and purification systems (NEB, USA) according to the manufacturer's instructions and MBP tag was cleaved off by factor Xa digestion. Concentration of protein was recorded at OD_{595} by the Bradford method using bovine serum albumin (BSA) as a standard. Protein banding pattern at different steps of purification were visualized by 12% sodium dodecyl sulfate-polyacrylamide gel electrophoresis (SDS-PAGE).

2.9. Functional assays

2.9.1. Dehydroascorbic (DHA) reductase assay

The DHA reductase activity of rHaGrx1 was assayed by the direct spectrophotometric method mentioned by Wells et al. and Stahl et al. [20,42]. Briefly, a series of 200 μL of a reaction mixture containing 200 mM sodium phosphate buffer (pH 6.9), 1 mM EDTA, 2 mM reduced L-Glutathione (GSH) (Sigma, USA), and 25 μg/mL of rHaGrx1 was prepared in order to perform kinetic analysis for rHaGrx1 with respect to DHA concentration. The reaction was initiated by adding a series of DHA solutions with varying concentrations (0, 0.5, 1, 1.5, and 2 mM) (Sigma, USA). Initial and final absorbance was measured at 265 nm with 2-min intervals. rHaGrx1 kinetic activity with respect to GSH concentration was measured using 25 μg/mL of rHaGrx1, 1.5 mM DHA, and a series of GSH solutions with varying concentrations (0, 0.5, 1, 1.5 and 2 mM). A blank without protein was simultaneously run for each reaction in order to eliminate background error occurred by any nonenzymic reaction between GSH and DHA. All spectrophotometric data were obtained by the SYNERGY/HT™ microplate reader (Biotek, Korea). The experiment was performed in triplicate at 25 °C. The Michaelis-Menten constant (K_m) and turnover number (K_{cat}) were determined using the Lineweaver-Burk plot [43].

2.9.2. Relative DHAR activity of HaGrx1 with different thiol compounds

The impact of different thiol compounds on Grx1 activity was measured as described previously with slight modifications [44]. Reduced GSH, 1,4-dithiothreitol (DTT), L-cysteine, and 2-mercaptoethanol (all from Sigma-Aldrich, USA) were used as thiol compounds. The dehydroascorbic reduction assay was performed as described in section 3.4.1 using 12.5 μg/mL rHaGrx1 protein, 0.5 mM DHA and 2 mM thiol compound. The HaGrx1 activity in the presence of the different thiol compounds was calculated relative to HaGrx1 activity with GSH as 100%. Relative HaGrx1 activities were statistically compared ($p < 0.05$) using Kruskal–Wallis one-way analysis of variance test using IBM SPSS 24 software.

2.9.3. β-Hydroxyethyl disulfide (HED) and reduction assay

HED reduction activity of rHaGrx1 was assayed as described

Table 1
Primers used for cloning and quantitative real-time PCR.

Primer Name	Sequence 5′–3′	Description
HaGrx1 qPCR forward	GCGCGTCAAGACATGAATAG	T_m 61 °C, 139 bp
HaGrx1 qPCR reverse	CCAGTTTGCCACTCTTATGC	T_m 60 °C, 139 bp
HaGrx1 cloning forward	GAGAGAgatatcATGGCTCAGCAATTCGTCCAGGCTAAAA	T_m 59.9 °C, 436 bp, *Eco*RV
HaGrx1 cloning reverse	GAGAGAgaattcTCACTGGAGAACCCCAATGGACT	T_m 60 °C, 436 bp, *Eco*RI
40S ribosomal S7 forward	ACTCTGGAACTGGCAGAGGAAGAC	T_m 60 °C, 187 bp
40S ribosomal S7 reverse	TGAAGTCATTCATGTTGGTGGCCTGTA	T_m 60 °C, 187 bp

previously by measuring the decrease in absorbance at 340 nm [37,38]. For the kinetic analysis of GSH, the reaction was performed in a 500-μL reaction mixture containing 100 mM Tris-HCl (pH 7.9), 0.2 mM NADPH, 2 mM EDTA, 0.1 mg/mL bovine serum albumin, 0.1 μg/mL glutathione reductase, 0.7 mM HED, and different GSH concentrations (0.2–2 mM). After adding HED, the absorbance was measured for 3 min (30-sec intervals) in order to confirm the termination of the nonenzymic spontaneous reaction between HED and GSH. Then, 0.19 μM rHaGrx1 was added to initiate the enzymatic reaction and the absorbance at 340 nm was recorded for 2 min. Similarly, kinetic analyses for HED were determined using varying concentrations of HED (0.3–1.8 mM) in the presence of 1 mM GSH and 0.19 μM rHaGrx1. K_m and K_{cat} values were calculated by the Lineweaver-Burk plot method.

2.9.4. Turbidimetric assay of insulin disulfide reduction

The rate of insulin disulfide reduction by rHaGrx1 was monitored spectrophotometrically at 650 nm as described previously [45]. The 200-μL reaction mixture contained 0.1 M potassium phosphate buffer (pH 7.9), 0.13 mM bovine insulin, 2 mM EDTA, and different concentrations of rHaGrx1 (2–17 mM). The reaction was initiated by adding 1 mM GSH as a reductant. The treatments were statistically compared ($p < 0.05$) with 0 μg/mL protein + GSH control by independent Student's t-test using IBM SPSS statistics 24 software.

3. Results

3.1. Sequence analysis of HaGrx1

The length of the coding sequence of HaGrx1 (Accession No. MK078310) was 321 bp and encoded a protein with 106 amino acids (aa). The theoretical isoelectric point (pI) and molecular mass of the deduced HaGrx1 protein were 7.71 and 11.77 kDa, respectively. HaGrx1 does not contain any signal peptides or N-linked glycosylation sites. According to the NCBI conserved domain database, HaGrx1 consists of a glutaredoxin conserved domain (14–98 aa) and belongs to the thioredoxin-like superfamily. Further, it contains a CSYC (23–26 aa) active site which represents the conserved CXXC thioredoxin/glutaredoxin catalytic motif. Moreover, HaGrx1 has 11 GSH binding sites as depicted in Fig. 1.

The predicted tertiary model for HaGrx1 covers 77% of the protein's 3D structure (Fig. 2). Further, it showed a typical Grx tertiary structure with five α-helixes and four β-sheets. According to the multiple sequence alignment (Fig. 3A), an active CXXC motif was conserved for all selected Grx1 orthologs. Further, many of the GSH binding sites that can be found in HaGrx1 were conserved in other Grx1 orthologs.

The deduced HaGrx1 shares the highest identity (97.2%) with Grx1 homologs of *Hippocampus comes* followed by *Labrus bergylta* (Table 2). Further, HaGrx1 shared 57.5% sequence identity and 72.6% similarity with the Grx1 homolog from *Homo sapiens*. According to the phylogenetic reconstruction (Fig. 3B), glutaredoxins are universally distributed in all the living organisms including bacteria, plants, and animals. HaGrx1 was in a clade with other fish Grx1 counterparts while closely clustered with the *H. comes* Grx1 ortholog (Fig. 3B).

3.2. Tissue distribution and immune challenge

As depicted in Fig. 4A, *HaGrx1* was ubiquitously expressed in all the 14 tissues tested. The highest expression of *HaGrx1* was observed in muscle, followed by the ovary, whereas the lowest expression was observed in the skin.

According to the temporal expression in the blood (Fig. 4B), significant modulations of *HaGrx1* were observed upon treatment with selected PAMPs and live bacteria. *HaGrx1* was significantly upregulated early as 3 h p.i. against LPS challenge and the significant upregulation was observed at 72 h p.i. *HaGrx1* transcription in response to *E. tarda* showed the highest expression at 3 h p.i. and upregulation lasted for 48 h p.i. *HaGrx1* expression against *S. iniae* showed early upregulation at 3–6 h p.i. For poly I:C, significant *HaGrx1* expression was observed at 3, 12, and 72 h p.i.

3.3. Expression and purification of rHaGrx1

According to the SDS PAGE gel image (Fig. 5, lane 6), rHaGrx1-MBP fusion protein can be identified as a single band between 50 kDa and 70 kDa. The approximate size of the rHaGrx1-MBP fusion protein is 54 kDa. The band present in the Lane 7 (Fig. 5), represented the predicted molecular weight of rHaGrx1 (11.77 kDa) after the factor Xa digestion.

3.4. Functional studies

3.4.1. Dehydroascorbic (DHA) reduction assay

The dehydroascorbic reduction activity of rHaGrx1 was analyzed using 25 μg/mL protein. The rHaGrx1 showed significant DHA reduction activity with compared to the control. As seen in Fig. 6A, the DHA reduction activity of rHaGrx1 increased linearly up to 1.5 min with 0.5–2 mM DHA concentrations at constant GSH concentration. The DHA reduction activity of rHaGrx1 increased linearly up to 2 min with 0.5–2.0 mM GSH at constant DHA concentrations (Fig. 6B). Kinetic analysis of the DHA reduction activity of rHaGrx1 revealed apparent K_m and K_{cat} values with respect to each substrate that is shown in Table 3.

3.4.2. Relative DHAR activity of HaGrx1 with different thiol compounds

Since various thiol compounds may activate the Grx, the DHAR activity of rHaGrx1 was determined using four reducing thiol compounds. HaGrx1 showed the highest DHAR activity in the presence of DTT as the reductant thiol compound (Fig. 6C). The DHAR activity of HaGrx1 differed in order of DTT > GSH > 2-ME > L-cysteine with the thiol compounds.

3.4.3. HED reduction assay

The small molecular weight disulfide reduction activity of rHaGrx1 was analyzed by HED assay. rHaGrx1 showed significant disulfide reduction activity with different GSH concentrations. HED reduction activity of rHaGrx1 was increased in a GSH concentration-dependent manner at a constant HED concentration (Fig. 7). The apparent $K_{m,}$ and K_{cat} with respect to GSH were cited in Table 3.

3.4.4. Turbidimetric assay of insulin disulfide reduction

Insulin disulfide reduction assay was performed to evaluate the oxidoreductase activity of rHaGrx1. According to data shown in Fig. 08, significant insulin reduction activity was observed upon 5 min in GSH + rHaGrx1 treated samples. Higher insulin reduction activity was observed in the 200 μg/mL rHaGrx1 + GSH sample compared to lower concentrations of rHaGrx1 + GSH. However, disulfide reduction activity was not detected within the observed incubation period for rHaGrx1 in the absence of GSH. Further, samples containing only GSH showed lower absorbance compared to those of the rHaGrx1 + GSH treated samples.

4. Discussion

Redox-active thiol-containing proteins such as Trx and Grx play a vital role in redox homeostasis which leads to scavenging of reactive oxygen species (ROS). ROS accumulation causes various pathological conditions and consequently leads to cell damage and apoptosis [46]. There are many studies on Grx1 orthologs from different species including viruses [10], bacteria [18], fungi [5], plants [47], and mammals [48], but few functional studies from fish species regarding innate immunity and oxidative stress. In this study, characteristics of HaGrx1 were evaluated based on *in-silico* analysis, innate immune responses, and redox activity.

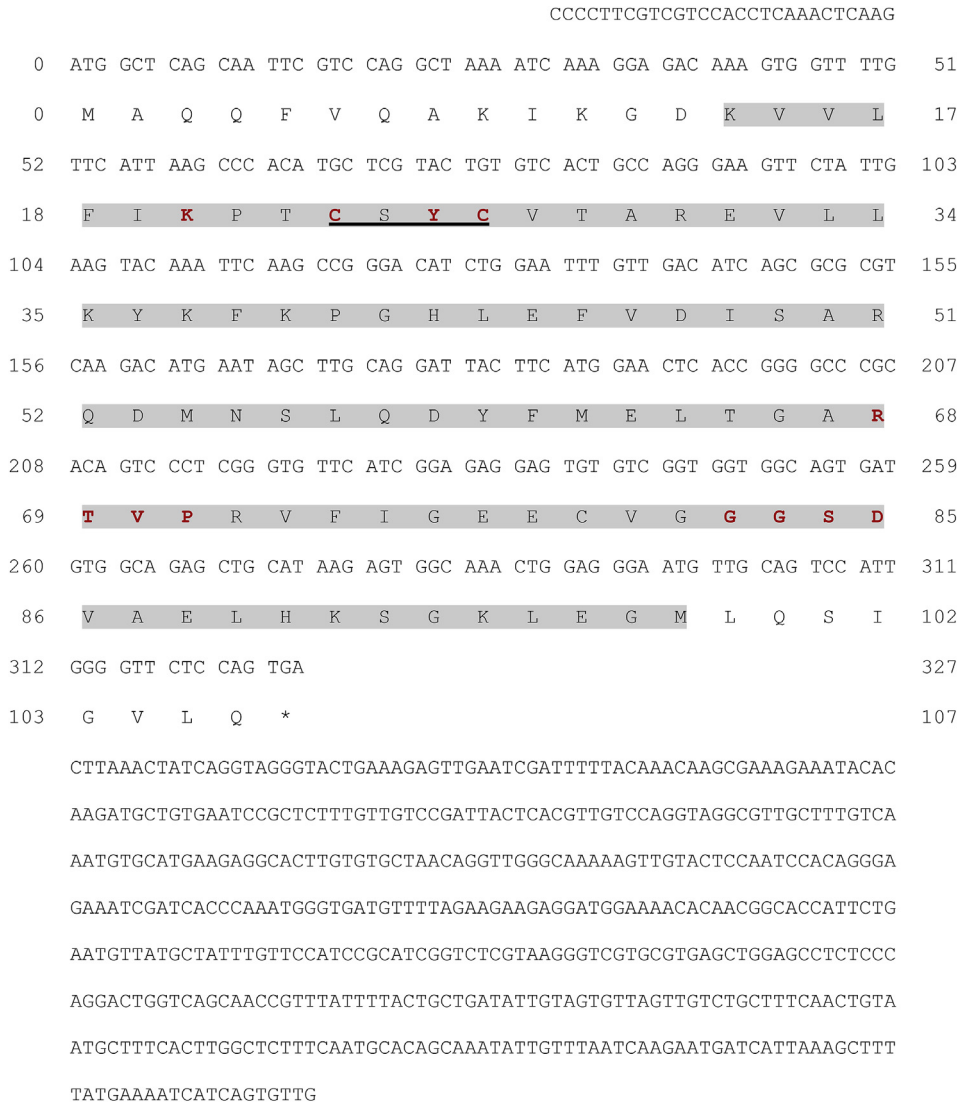

Fig. 1. Nucleotide and deduced amino acid sequence of HaGrx1 from *Hippocampus abdominalis*. The predicted glutaredoxin domain is shaded in gray and the conserved CXXC motif is marked with underlined bold red letters. The GSH binding sites of the protein sequence are indicated in bold black letters. The stop signal of the protein is denoted by an asterisk. (For interpretation of the references to color in this figure legend, the reader is referred to the Web version of this article.)

The deduced HaGrx1 protein sequence possessed similar characteristics to those of Grx1 from other species. For example, human Grx1 showed identical features to HaGrx1 [49]. Further, the molecular mass of human Grx1 and HaGrx1 is 11.76 and 11.77 kDa, respectively. *E. coli* Grx also has similar features such as a molecular weight of 10 kDa and a CXXC active site [3]. Therefore, the structure of Grxs appeared to be conserved to both eukaryotes and prokaryotes. HaGrx1 has 11 GSH binding sites that are essential for its function. Usually, GSH acts as an electron donor for many proteins such as Grx, Glutathione *S*-transferase (GST), and Glutathione reductase (GR). Therefore, GSH binding sites are essential for the redox function of such proteins. Among the 11 GSH binding sites in HaGrx1, nine residues are highly conserved in vertebrates, whereas all 11 residues are conserved and represented by the same amino acid in fish Grx1 orthologs (Fig. 3A). Hence, HaGrx1 may be classified as a glutaredoxin with typical sequence characteristics. However, the CXXC catalytic motif is commonly represented as CPYC in other species, but HaGrx1 contains CSYC residues, which can also be observed in some fish species (Fig. 3A). According to Foloppe et al., redox activity of the CXXC motif in *E. coli* can be greatly affected by alterations in -X-X- residues [50]. Therefore, alteration of CPYC to CSYC can change the redox properties of the HaGrx1 sequence. This point can be further emphasized by the fact that human Grx2, which contains CSYC, has the ability to obtain electrons from mitochondrial thioredoxin reductase and coordinating Fe/S clusters [50]. Further, alterations in peripheral amino acids can greatly affect the redox potential [50]. Therefore, HaGrx1 may possess different catalytic properties from all other Grx1 orthologs.

The tertiary structure of HaGrx1 showed 77% similarity to human Grx1 PDB template, suggesting that it has a typical Grx1 3D structure. HaGrx1 also has a typical thioredoxin fold, which is conserved in enzymes that catalyze disulfide bond formation and isomerization. The spatial topology of the thioredoxin fold comprises central four antiparallel β-sheets surrounded by three α-helixes [51]. However, HaGrx1 was found to consist of 5 α-helixes. It has been reported that most prokaryotic Grxs contain a typical thioredoxin structure, but some eukaryotic Grxs possess two additional α-helixes on the N- and C-termini [52]. Due to the conserved structural features, HaGrx1 showed 57.5% identity with human Grx1 amino acid sequence, but according to data shown in Fig. 3B and phylogenetic reconstruction, HaGrx1 is more closely related to fish Grx1 orthologs. Moreover, HaGrx1 shows the highest homology with Grx1 from *H. comes*. Therefore, the *in-silico* analysis results in this study provide clear evidence of the evolutionary link and the ancestral lineage of HaGrx1 to other Grx1 orthologs.

The conservation of Grx structure and function throughout all

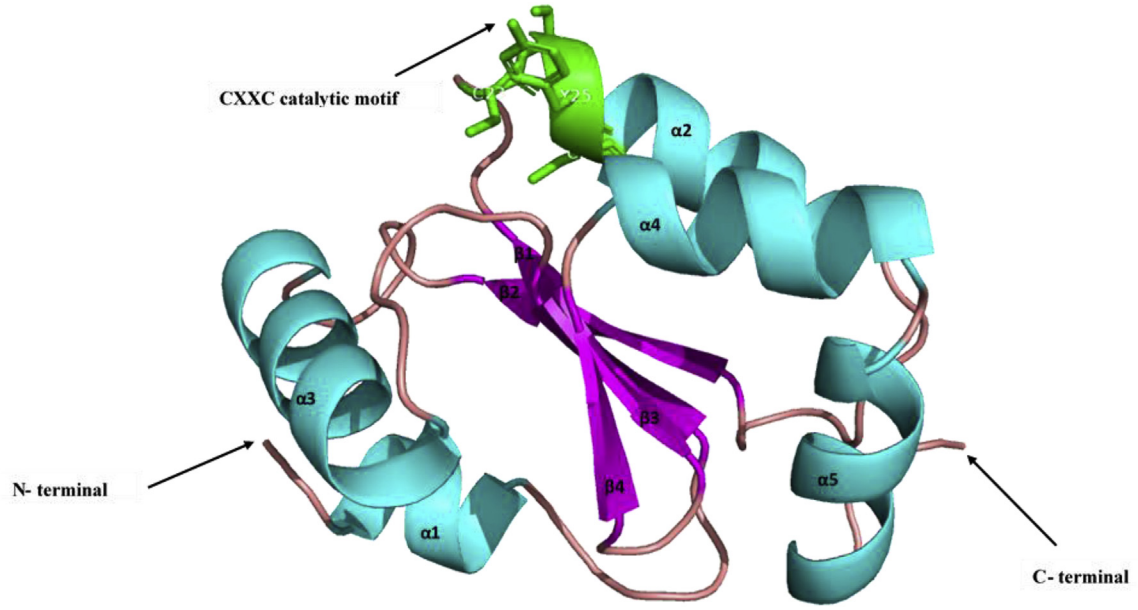

Fig. 2. Predicted tertiary structure of HaGrx1.

organisms, even plants and viruses, denotes the importance of its functions for biological processes. The most well-elucidated function of Grx1 is its role in regulating redox homeostasis, which has great influence on immune, metabolic, and hormonal functions [53]. The antioxidant activity of Grx is exerted by an enzymatic system comprised of GSH, glutathione reductase (GR), and NADPH [54]. Grx is a key reducing agent present in cells that can catalyze the activity of a versatile range of substrates. By catalyzing these substrates, Grx1 regulates many metabolic and signaling pathways, and thus is recognized as a transcription factor for many genes such as Bcl-2, Bcl-xL, and apurinic (apyrimidinic) endonuclease/redox-factor 1 (APE/Ref-1) [11].

Further, it is reported that the redox activity of Grx1 can functionally overlap with the activity of many proteins. For instance, it catalyzes many substrates utilized by Trx such as insulin and ribonucleotide reductase [55]. Further, it possesses dehydroascorbic reductase activity, glutathione peroxidase activity, and glutathione *S*-transferase activity [3,20,56]. Most importantly, Grxs are involved in Fe/*S* cluster coordination in cells [1]. Hence, Grx1 can be recognized as a multifunctional enzyme, thereby ubiquitous expression in tissues can be expected. The tissue-specific expression of *HaGrx1* also exhibited ubiquitous expression in all the tissues examined and the highest significant expression was observed in muscle. ROS are highly generated in muscles due to the high energy production and utilization of this tissue [57]. Seahorses are tiny sea creatures with characteristic skeletal and muscle structures required for swimming and to anchor to substrates [27]. They have a strong prehensile tail that attaches to substrates and a large dorsal fin that exerts propulsive force to swim in an upright position [27]. Therefore, muscles attached to fins and the skeleton are highly active, and ROS generation can be increased in this tissue. The highest expression of *HaGrx1* in muscle suggests its requirement for ROS neutralization. The second highest expression was observed in the ovary followed by brain tissue (Fig. 4A). Ovaries are metabolically active and undergo various stresses [58]. Fernández et al. reported that Grx1 expression in rat ovary significantly influences the maturation of oocytes and survival of luteal cells by protecting them from apoptosis and oxidative damage [13]. As female seahorses produce more than 1500 eggs/clutch, ovaries are highly active [25]. Therefore, significant *HaGrx1* production in this tissue suggests that it protects eggs from oxidative stress during maturation. Also, Grxs are intensively investigated upon protecting the central nervous system from oxidative stress [15,16,22]. Further, it is reported that Grx protects cerebellar granule neurons from dopamine-induced apoptosis by activating NF-κB [15]. Ascorbic acid is one of the key antioxidant molecules needed for several functions of the central nervous system, including the maturation and differentiation of neurons, myelin formation and synthesis of catecholamine [59]. Therefore, significant tissue-specific expression of HaGrx1 in the brain may be evidence that antioxidant function is required for the recovery of ascorbic as well as the elimination of ROS, which can cause neurodegeneration.

Grxs plays an important antioxidant role in the blood as red blood cells are highly exposed to xenobiotics and ROS formed during inflammation. Therefore, vertebrate RBCs have their own reactive sulfhydryl groups on each β subunit and they can exert antioxidant activity against free radicals such as H_2O_2 [60,61]. However, oxidation of these SH- groups can affect the oxygen- and heme-binding capacity of the RBCs [62]. Therefore, it is reported that Grx in erythrocytes has a distinct function in regenerating oxidized SH groups on RBCs [62]. On the other hand, it is reported that erythrocytes have a bactericidal effect by producing ROS against pathogens [63]. Thus, it is important to regulate ROS production to a proper level to avoid causing cell damages. As a result, expression of Grx1 in blood during pathogenic infection is important in many ways. The significant modulation of *HaGrx1* transcripts in blood upon exposure to pathogens such as *E. tarda* and *S. iniae* suggests both sulfhydryl homeostasis and ROS neutralization. In addition, Grx1 can activate IL-1 and TLR-4 signaling pathway by regulating TRAF6 [64]. IL-1 is a proinflammatory cytokine that promotes activation of immune cells such as macrophages, monocytes, lymphocytes, and neutrophils [65]. TLR-4 also acts as a receptor for LPS and regulates the secretion of proinflammatory factors [66]. Both IL-1 and LPS activate myeloid differentiation factor 88 and TRAF6 and thus promote proinflammatory signaling cascades as an innate immune response [65,66]. TRAF6 is deglutathionylated by Grx1 upon IL-1 induction and it can activate the NF-κB pathway [64]. Further, Grx1 can promote the auto-polyubiquitination of TRAF6, which subsequently activates NF-κB [64]. These proinflammatory pathways are highly active during immune stimulation. Therefore, significant upregulation of *HaGrx1* in blood upon exposure to LPS, *E. tarda,* and *S. iniae* can indicate the activation of proinflammatory pathways by deglutathionylation of TRAF6. Poly I:C is a synthetic compound analog to viral dsRNA. It can activate IRF3 through the TLR3 signaling cascade. IRF3 is a key transcription regulatory factor of antiviral interferon genes. During viral infections, IRF3 translocates to the nucleus and

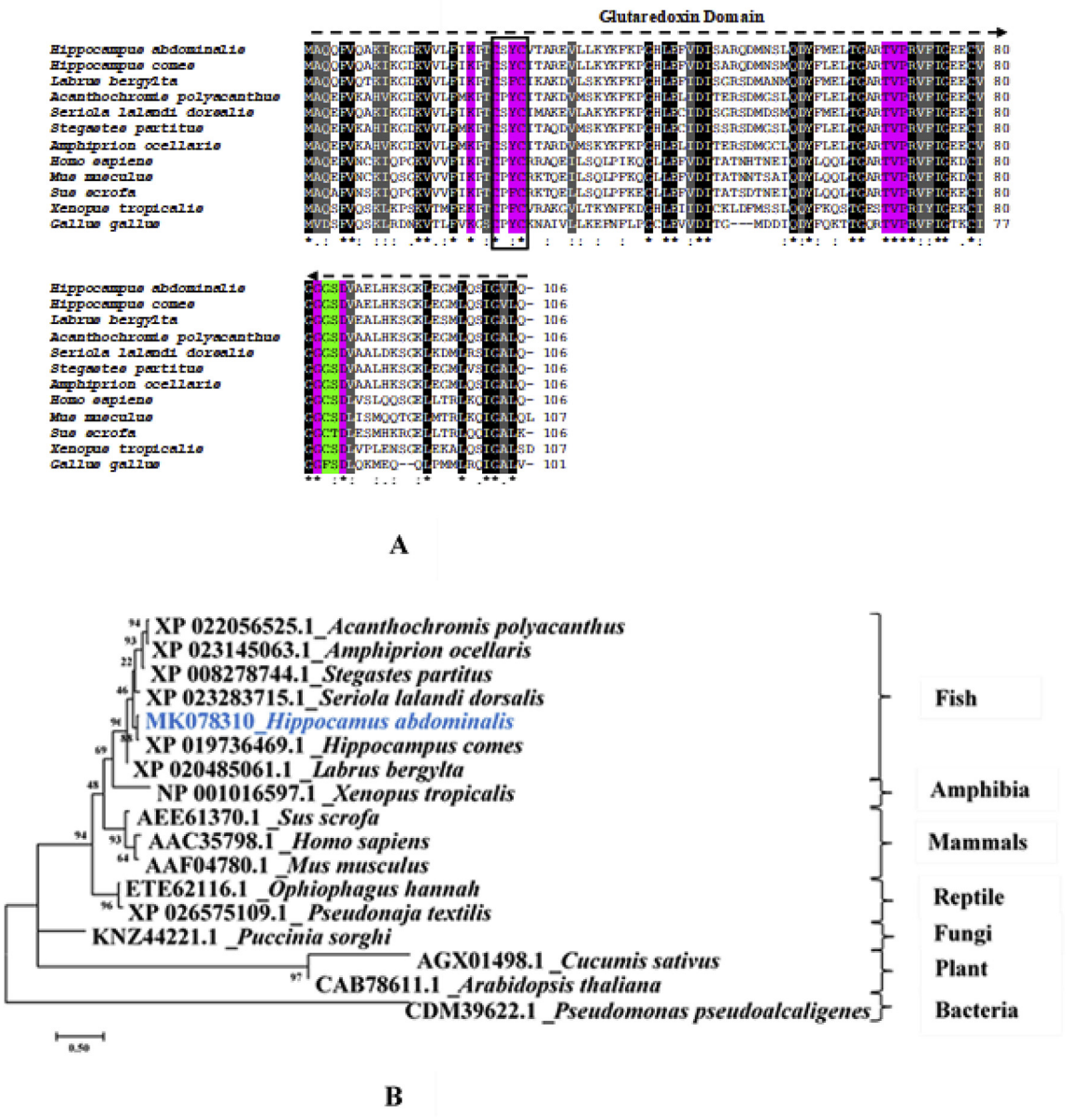

Fig. 3. (A) Multiple-sequence alignment of HaGrx1 and its orthologs from selected organisms. Sequence alignments were obtained using the Clustal Omega tool. Conserved residues are shaded in black and semi-conserved residues are shaded in gray. The conserved CXXC motif is marked with a black box and GSH binding sites that are conserved in HaGrx1 and all other selected organism are shaded with a purple color. GSH binding sites that are conserved only in selected fish species are marked with green color. Accession numbers of selected protein sequences are listed in Table 2(B) Phylogenetic reconstruction of HaGrx1. The evolutionary development of HaGrx1 was analyzed with its different homologs categorized under different taxonomic groups based on the multiple alignment profiles of the protein sequences generated by the Maximum likelihood method using MEGA 7.0 software. Bootstrap support values corresponding to each branch are indicated. (For interpretation of the references to color in this figure legend, the reader is referred to the Web version of this article.)

Table 2
Identity and similarity percentages of Grx1 orthologs from different species compared to HaGrx1.

Accession No	Scientific name	Identity (%)	Similarity (%)
XP_019736469.1	*Hippocampus comes*	97.2	100.0
XP_020485061.1	*Labrus bergylta*	84.0	90.6
XP_023283715.1	*Seriola lalandi dorsalis*	83.0	91.5
XP_008278744.1	*Stegastes partitus*	82.1	92.5
XP_023145063.	*Amphiprion ocellaris*	82.1	91.5
XP_020485061.1	*Acanthochromis polyacanthus*	81.1	91.5
AAC35798.1	*Homo sapiens*	57.5	72.6
AEE61370.1	*Sus scrofa*	57.5	73.6
NP_001016597.1	*Xenopus tropicalis*	57.0	70.1
AAF04780.1	*Mus musculus*	54.2	73.8
CAA70437.1	*Gallus gallus*	47.2	67.0

activate transcription. Deglutathionylation of IRF3 is essential to activate IRF3 and the gene expression of IFNβ. Prinarakis et al. reported that deglutathionylation of IRF3 is regulated by cytoplasmic Grx1 in humans. Therefore, Grx1 plays a crucial role in controlling the cell signaling pathway upon viral infection. The significant upregulation of HaGrx1 against Poly I:C may be evidence of activation of IRF3 by deglutathionylation. The aforementioned proinflammatory signaling pathways are important for innate and adaptive immunity of higher organisms, including the seahorse. *E. tarda* and *S. iniae* can cause severe infections in a broad range of animals. *HaGrx1* transcriptional profiles against immune stimulants exhibits overall upregulation patterns but significant downregulations was observed at time point of 24 h p.i. The reason for the downregulations is not clear but Grx1 can be involved in dynamic regulation of NF-κB during the infections and oxidative stress.

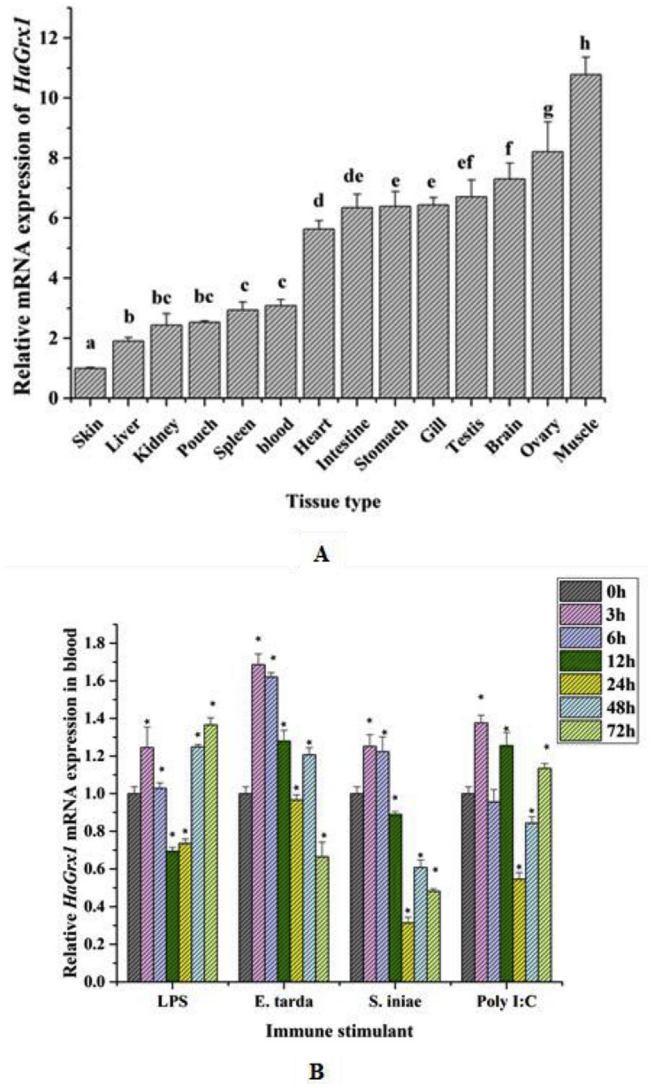

Fig. 4. (A) Tissue-specific expression of *HaGrx1* under normal physiological conditions. The Livak method was used to calculate the relative mRNA expression of each tissue, and seahorse 40S ribosomal protein S7 gene was used as an internal control gene in the qPCR experiment. The data are represented as mean values (n = 3) ± standard deviation (S.D.). (B) Temporal expression profiles of *HaGrx1* in the blood after PAMP (LPS and poly I:C) and bacterial *(Edwardsiella tarda* and *Streptococcus iniae)* challenges. The Livak method was used to calculate the fold changes in mRNA expression, and seahorse 40S ribosomal protein S7 gene was used as an internal control gene in the qPCR experiment. The relative fold changes in expression were compared with those of the PBS-injected control at different time points. The data are represented as mean values (n = 3) ± S.D. Significant differences compared to the blank (0 h) are indicated with an asterisk for $P < 0.05$.

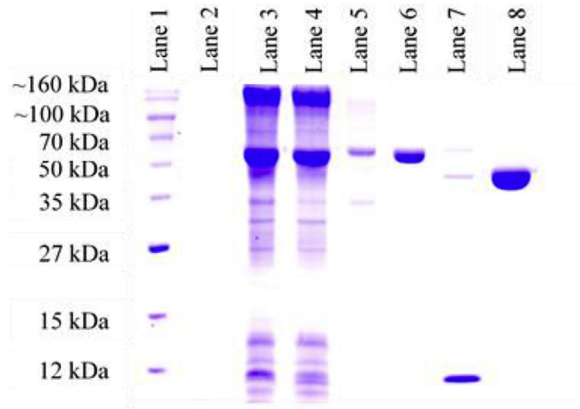

Fig. 5. SDS-PAGE analysis of overexpressed and purified HaGrx1 as an MBP-fusion protein. Lane 1: unstained protein ladder, Lane 2: crude extract of un-induced *E. coli* C2327 cells, Lane 3: crude extract of induced *E. coli* C2327, Lane 4: supernatant after sonication and centrifugation of induced *E. coli* C2327 cells, Lane 5: Pellet, Lane 6: purified HaGrx1 fusion protein, Lane 7: cleaved rHaGrx1 by factor Xa, Lane 8: Purified MBP protein.

Reynaert et al. suggested that key immune regulatory factor NF-κB is known as redox sensitive molecule and Grx1 can modulate the magnitude of activation of the NF-κB through Grx1 dependent deglutathionylation of IKK-β. Therefore, Grx1 may modulate the extent and timing of activation of NF-κB signaling. They also suggested that modulation of NF-κB and IKK-β upon oxidative and inflammatory responses is a protective mechanism to avoid irreversible inactivation of IKK-β and to ensure rapid regeneration of enzymatic activity [67]. Therefore, the dynamic upregulations and downregulations observed in this study might reflect the potential involvement of HaGrx1 in regulation of NF-κB signaling cascade through its differential expression patterns.

Ascorbic acid (AA) is a highly required cofactor for many enzymes as involved in the biosynthesis of collagen, creatinine, catecholamine, and peptide hormones [59]. Further, they terminate free radical chain reactions by scavenging ROS and reactive nitrogen species (RNS). During the above biological processes, AA can be oxidized into DHA which can be used to regenerate AA again [42]. The conversion of DHA to AA is mainly catalyzed by GSH-dependent DHA reductase, but some other enzymes such as thioredoxin reductase, Grx, and GST-omega also possess dehydroascorbate reductase (DHAR) activity [68–70]. Similarly, HaGrx1 also demonstrated DHAR activity. As shown in Table 3, the K_m value of DHA is lower than the K_m of GSH. Higher K_m value indicates that a high substrate level is required to reach the V_{max}. As HaGrx1 has 11 GSH binding sites, the K_m for GSH can be increased. According to the literature, HaGrx1 shows a similar K_m value to that of bovine thymus glutaredoxin upon DHA and GSH exposure [20]. The catalytic efficiency (V_{max}/K_m) of HaGrx1 for DHA is higher than that of Grx1 from *Chlamydomonas reinhardtii* [45], indicating that HaGrx1 has better redox properties.

Grxs can utilize thiol compounds other than GSH [44,71]. Therefore, we analyzed the DHAR activity of rHaGrx1 with different thiol compounds. Interestingly, the highest relative DHAR activity of rHaGrx1 was observed with DTT. In a prior study, Grxs showed the best activity with GSH as reductant compound [2]. However, another study reported that Grxs have better activity with DTT in assays, including the insulin reductase assay [72]. DTT has two SH groups and is considered a strong electron donor or reductant [73]. It is commonly used in *vitro* assays of Trx, but is not considered a naturally available compound in cells [74]. L-cysteine is a sulfur-containing non-essential amino acid, which can act as a reducing agent [75]. L-cysteine may also act as a disulfide reducing agent and its activity is lower than GSH [76]. Our results mirror these prior observations. β-mercaptoethanol is a reducing agent that is used in several enzymatic assays due to its excellent ability to inhibit oxidation of free sulfhydryl residues. According to our results, β-mercaptoethanol was not a good reducing agent for rHaGrx1 upon DHAR activity. The nature of the selective activity of Grxs on different thiol compounds remains unclear.

HED is a synthetic compound used as the standard substrate for Grxs. According to the elucidated mechanistic model, HED initially reacts with GSH nonenzymatically to yield a mixed disulfide between GSH and 2-mercaptoethanol (GSSEtOH) [77]. Therefore, GSSEtOH is the actual substrate for Grx in the HED assay. The CXXC motif of Grx1 serves as SH- groups (thiol groups) that can attack GSSEtOH during the oxidative half-reaction. Subsequently, GSSEtOH reduces to 2-mercaptoethanol and produces *S*-glutathionylated Grx. Glutathionylated Grx is

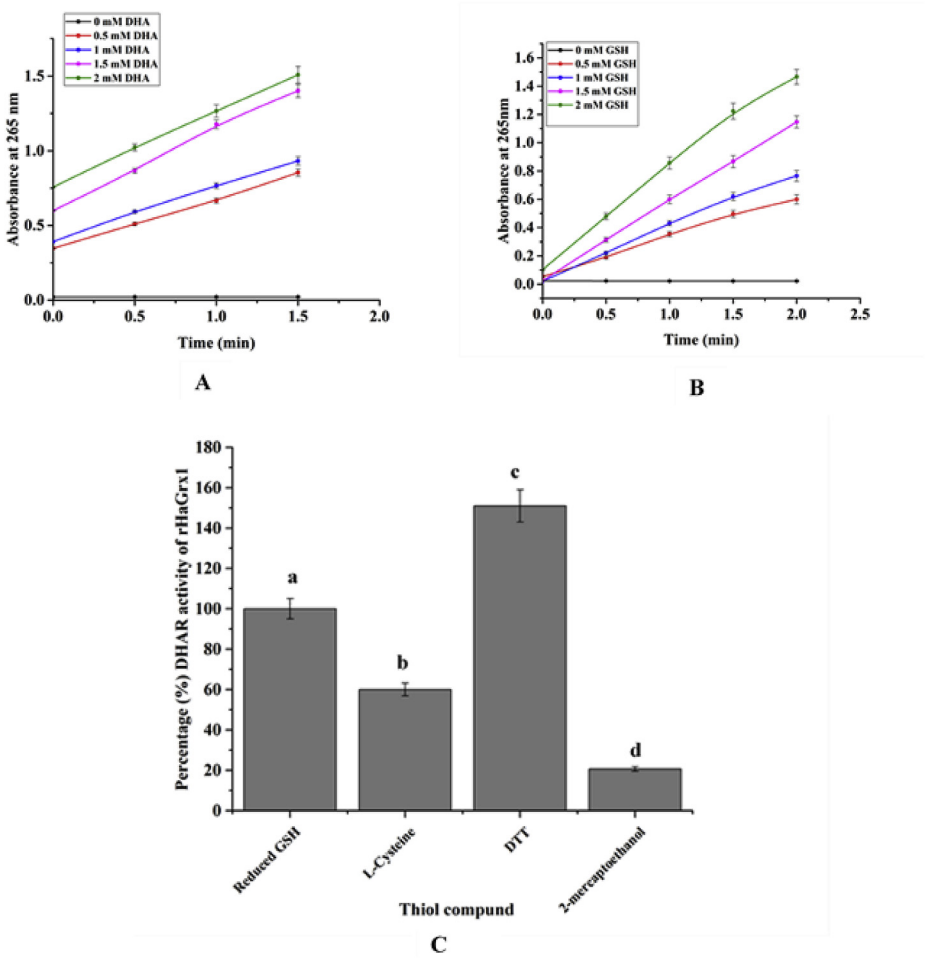

Fig. 6. (A) DHA reduction activity of rHaGrx1 with different DHA concentration and (B) with different GSH concentration. The data are represented as mean values (n = 3) ± S.D. (C) Dehydroascorbate reductase activity of rHaGrx1 with different reducing thiol compounds at 25 °C. The experiment was conducted in triplicates. The data represent percentage (mean ± S.D). Data with different letters are significantly different among each group ($p < 0.05$).

regenerated by an oxidative half-reaction with GSH, producing oxidized glutathione (GSSG). The subsequent reaction between NADPH and GSSG, catalyzed by GR, recovers the GSH, as well as NADPH consumption by GR, providing an indirect method to monitor GRX activity spectrophotometrically [78]. According to data shown in Table 3, HaGrx1 exhibited lower catalytic properties towards GSH compared to those of other Grx1 orthologs [20,79]. Johansson et al. reported that replacing the proline in CXXC with serine can reduce the catalytic properties compared to other Grx1s containing CPYC [80]. However, they reported that CSYC alteration in Grxs could increase the affinity toward the glutathionylated substrate, clarifying the behavior of HaGrx1 towards HED (Table 3).

Insulin is a two-chain heterodimer protein with two peptide chains. A and B chains of insulin are linked by disulfide bonds [81]. These interchain disulfide bonds can be reduced by proteins such as protein disulfide isomerase (PDI), Trx, and various other proteins [74]. During the insulin disulfide reduction, free A and B chains are precipitated and turbidity can be measured at 650 nm [74]. Though some reports suggest that glutaredoxin is not effective in insulin disulfide reduction, some studies reported that Grx could exhibit lower insulin reduction activity compared to thioredoxin in the presence of GSH as an electron donor [45,72]. According to data shown in Fig. 8, HaGrx1 also showed concentration-dependent insulin disulfide reduction activity. However, HaGrx1 displayed lower absorbance values at 650 nm compared to thioredoxin proteins from *Hippocampus abdominalis* [82].

In conclusion, the *HaGrx1* gene was identified in this study and subjected to various molecular, transcriptional, and functional analyses. HaGrx1 possesses a typical Grx1 structure with a CSYC thioredoxin motif. Spatial and temporal expression analysis showed that *HaGrx1* was constitutively expressed in all the seahorse tissues examined and significantly upregulated in response to LPS, poly I:C, *S. iniae,* and *E. tarda* immune stimulations. Further, HaGrx1 exhibited reductive activity toward DHA, insulin, and HED. Therefore, HaGrx1 could be actively involved in suppressing oxidative stress from both abiotic and

Table 3
Kinetic parameters of rHaGrx1 for DHA and HED assays at 25 °C. The experiment was conducted in triplicates and data represent mean ± S.D.

	DHA assay		HED assay	
Substrates	GSH	DHA	GSH	HED
K_m (mM)	1.56 ± 0.132	0.57 ± 0.154	3.21 ± 0.875	0.21 ± 0.032
K_{cat} (s^{-1})	4.86 ± 0.186	4.62 ± 0.321	18.3 ± 0.86	48.8 ± 1.72
$K_{cat/km}$ ($M^{-1}s^{-1}$)	3.11×10^3	8.105×10^3	5.7×10^3	2.32×10^5

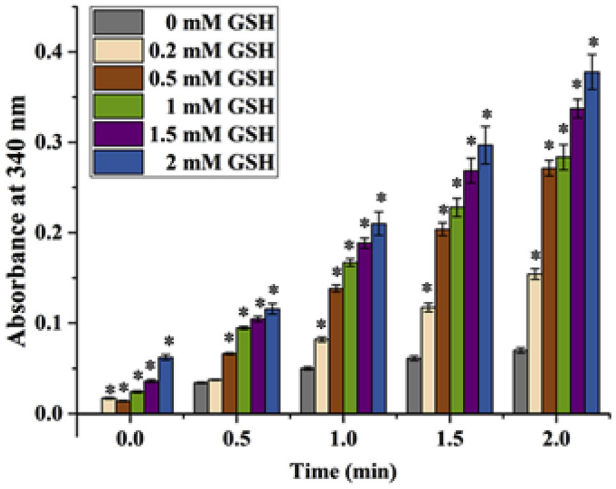

Fig. 7. HED reduction activity of rHaGrx1 with different GSH concentrations at 25 °C. Data were obtained from triplicate determinations and are expressed as mean values ± S.D. Significant differences compared to 0 mM GSH are indicated with "*" ($p < 0.05$).

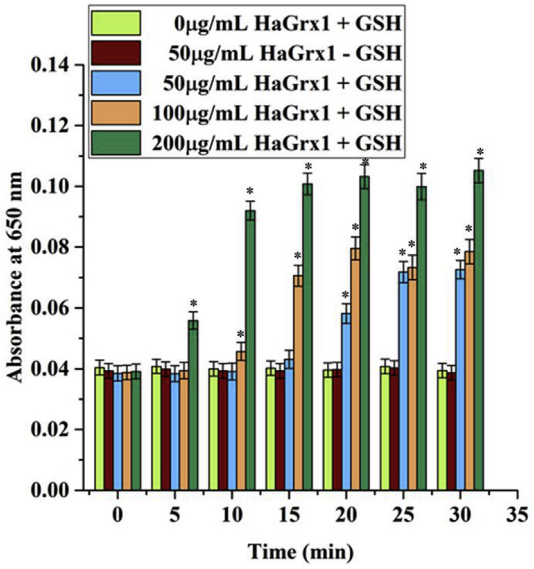

Fig. 8. Insulin disulfide reduction activity of rHaGrx1 with different protein and GSH combinations. The turbidity was measured in every 5 min incubation at 25 °C at 650 nm. Data was obtained from triplicate determinations and are expressed as mean values ± S.D. Significant differences ($p < 0.05$) compared to control (0 μg/mL rHaGrx1 + GSH) are indicated by *.

biotic sources. Altogether, the results in this study provide better knowledge about the role of HaGrx1 in the host defense system.

Acknowledgment

This research was supported by the 2019 scientific promotion program funded by Jeju National University and supported by the National Research Foundation of Korea (NRF) grant funded by the Korea government (MSIP) (NRF-2017R1C1B2008380).

References

[1] L. Bräutigam, C. Johansson, B. Kubsch, M.A. McDonough, E. Bill, A. Holmgren, C. Berndt, An unusual mode of iron-sulfur-cluster coordination in a teleost glutaredoxin, Biochem. Biophys. Res. Commun. 436 (2013) 491–496, https://doi.org/10.1016/j.bbrc.2013.05.132.
[2] A. Vlamis-Gardikas, A. Holmgren, Thioredoxin and glutaredoxin isoforms, Methods Enzymol. 347 (2002) 286–296, https://doi.org/10.1016/S0076-6879(02)47028-0.
[3] A.P. Fernandes, A. Holmgren, Glutaredoxins: glutathione-dependent redox enzymes with functions far beyond a simple thioredoxin backup system, Antioxidants Redox Signal. 6 (2004) 63–74, https://doi.org/10.1089/152308604771978354.
[4] C.H. Lillig, C. Berndt, A. Holmgren, Glutaredoxin systems, Biochim. Biophys. Acta - Gen. Subj. 1780 (2008) 1304–1317, https://doi.org/10.1016/j.bbagen.2008.06.003.
[5] E. Herrero, J. Ros, J. Tamarit, G. Bellí, Glutaredoxins in fungi, Photosynth. Res. 89 (2006) 127–140, https://doi.org/10.1007/s11120-006-9079-3.
[6] P. Haunhorst, C. Berndt, S. Eitner, J.R. Godoy, C.H. Lillig, Characterization of the human monothiol glutaredoxin 3 (PICOT) as iron-sulfur protein, Biochem. Biophys. Res. Commun. 394 (2010) 372–376, https://doi.org/10.1016/j.bbrc.2010.03.016.
[7] B. Selles, N. Rouhier, K. Chibani, J. Couturier, F. Gama, J.P. Jacquot, Chapter 13 glutaredoxin, The Missing Link between Thiol-Disulfide Oxidoreductases and Iron Sulfur Enzymes, first ed., Elsevier Ltd., 2009, , https://doi.org/10.1016/S0065-2296(10)52013-5.
[8] I. Rajagopal, B.Y. Ahn, B. Moss, C.K. Mathews, Roles of vaccinia virus ribonucleotide reductase and glutaredoxin in DNA precursor biosynthesis, J. Biol. Chem. 270 (1995) 27415–27418, https://doi.org/10.1074/jbc.270.46.27415.
[9] D.E. Hauwer, Identification Infection of Escherichia, 244 (n.d.) 6306–6309.
[10] D.A. Davis, F.M. Newcomb, D.W. Starke, D.E. Ott, J.J. Mieyal, R. Yarchoan, Thioltransferase (glutaredoxin) is detected within HIV-1 and can regulate the activity of glutathionylated HIV-1 protease in vitro, J. Biol. Chem. 272 (1997) 25935–25940, https://doi.org/10.1074/jbc.272.41.25935.
[11] M.M. Gallogly, M.D. Shelton, S. Qanungo, H. V Pai, D.W. Starke, C.L. Hoppel, E.J. Lesnefsky, J.J. Mieyal, Glutaredoxin regulates apoptosis in cardiomyocytes via NFkappaB targets Bcl-2 and Bcl-xL: implications for cardiac aging, Antioxidants Redox Signal. 12 (2010) 1339–1353, https://doi.org/10.1089/ars.2009.2791.
[12] M. Peltoniemi, Mechanism of Action of the Glutaredoxins and Their Role in Human Lung Diseases, (2007).
[13] R. González-Fernández, F. Gaytán, E. Martínez-Galisteo, P. Porras, C.A. Padilla, J.E. Sánchez Criado, J.A. Bárcena, Expression of glutaredoxin (thioltransferase) in the rat ovary during the oestrous cycle and postnatal development, J. Mol. Endocrinol. 34 (2005) 625–635, https://doi.org/10.1677/jme.1.01715.
[14] A. Stavreus-Evers, B. Masironi, B.M. Landgren, A. Holmgren, H. Eriksson, L. Sahlin, Immunohistochemical localization of glutaredoxin and thioredoxin in human endometrium: a possible association with pinopodes, Mol. Hum. Reprod. 8 (2002) 546–551.
[15] D. Daily, A. Vlamis-Gardikas, D. Offen, L. Mittelmani, E. Melamed, A. Holmgren, A. Barzilai, Glutaredoxin protects cerebellar granule neurons from dopamine-induced apoptosis by activating NF-κB via Ref-1, J. Biol. Chem. 276 (2001) 1335–1344, https://doi.org/10.1074/jbc.M008121200.
[16] Y. Takagi, T. Nakamura, A. Nishiyama, K. Nozaki, T. Tanaka, N. Hashimoto, J. Yodoi, Localization of glutaredoxin (thioltransferase) in the rat brain and possible functional implications during focal ischemia, Biochem. Biophys. Res. Commun. 258 (1999) 390–394, https://doi.org/10.1006/bbrc.1999.0646.
[17] J.J. Mieyal, S.A. Gravina, Thioltransferase is a specific glutathionyl mixed disulfide oxidoreductase, Biochemistry 32 (1993) 3368–3376, https://doi.org/10.1021/bi00064a021.
[18] A. Vlamis-Gardikas, F. Åslund, G. Spyrou, T. Bergman, A. Holmgren, Cloning, overexpression, and characterization of glutaredoxin 2, an atypical glutaredoxin from Escherichia coli, J. Biol. Chem. 272 (1997) 11236–11243, https://doi.org/10.1074/jbc.272.17.11236.
[19] F. Zahedi Avval, A. Holmgren, Molecular mechanisms of thioredoxin and glutaredoxin as hydrogen donors for mammalian S phase ribonucleotide reductase, J. Biol. Chem. 284 (2009) 8233–8240, https://doi.org/10.1074/jbc.M809338200.
[20] W.W. Wells, D.P. Xu, Y. Yang, P.A. Rocque, Mammalian thioltransferase (glutaredoxin) and protein disulfide isomerase have dehydroascorbate reductase activity, J. Biol. Chem. 265 (1990) 15361–15364.
[21] D.W. Starke, P.B. Chock, J.J. Mieyal, Glutathione-thiyl radical scavenging and transferase properties of human glutaredoxin (thioltransferase): potential role in redox signal transduction, J. Biol. Chem. 278 (2003) 14607–14613, https://doi.org/10.1074/jbc.M210434200.
[22] C. Berndt, G. Poschmann, K. Stühler, A. Holmgren, L. Bräutigam, Zebrafish heart development is regulated via glutaredoxin 2 dependent migration and survival of neural crest cells, Redox Biol 2 (2014) 673–678, https://doi.org/10.1016/j.redox.2014.04.012.
[23] L. Bräutigam, L. Schütte, Vertebrate-specific glutaredoxin is essential for brain development, SAVE Proc. 108 (2011) 20532–20537, https://doi.org/10.1073/pnas.1110085108.
[24] C. Mu, Q. Wang, Z. Yuan, Z. Zhang, C. Wang, Identification of glutaredoxin 1 and glutaredoxin 2 genes from Venerupis philippinarum and their responses to benzo[a]pyrene and bacterial challenge, Fish Shellfish Immunol. 32 (2012) 482–488, https://doi.org/10.1016/j.fsi.2011.12.001.
[25] A.C.J. Vincent, The international trade in seahorses, TRAFFIC Int (1996) 163, https://doi.org/10.1002/aqc.2493.
[26] H.J. Koldewey, K.M. Martin-Smith, A global review of seahorse aquaculture, Aquaculture 302 (2010) 131–152, https://doi.org/10.1016/j.aquaculture.2009.11.010.
[27] C. Woods, Aquaculture of the big-bellied seahorse Hippocampus abdominalis lesson 1827 (teleostei: syngnathidae), Thesis 1827 (2007) 251 http://researcharchive.vuw.ac.nz/handle/10063/288.
[28] M. Oh, N. Umasuthan, D.A.S. Elvitigala, Q. Wan, E. Jo, J. Ko, G.E. Noh, S. Shin, S. Rho, J. Lee, First comparative characterization of three distinct ferritin subunits from a teleost: evidence for immune-responsive mRNA expression and iron depriving activity of seahorse (Hippocampus abdominalis) ferritins, Fish Shellfish

Immunol. 49 (2016) 450–460, https://doi.org/10.1016/j.fsi.2015.12.039.
[29] R. Agarwala, T. Barrett, J. Beck, D.A. Benson, C. Bollin, E. Bolton, D. Bourexis, J.R. Brister, S.H. Bryant, K. Canese, C. Charowhas, K. Clark, M. Dicuccio, I. Dondoshansky, S. Federhen, M. Feolo, K. Funk, L.Y. Geer, V. Gorelenkov, M. Hoeppner, B. Holmes, M. Johnson, V. Khotomlianski, A. Kimchi, M. Kimelman, P. Kitts, W. Klimke, S. Krasnov, A. Kuznetsov, M.J. Landrum, D. Landsman, J.M. Lee, D.J. Lipman, Z. Lu, T.L. Madden, T. Madej, A. Marchler-Bauer, I. Karsch-Mizrachi, T. Murphy, R. Orris, J. Ostell, C. O'sullivan, A. Panchenko, L. Phan, D. Preuss, K.D. Pruitt, K. Rodarmer, W. Rubinstein, E. Sayers, V. Schneider, G.D. Schuler, S.T. Sherry, K. Sirotkin, K. Siyan, D. Slotta, A. Soboleva, V. Soussov, G. Starchenko, T.A. Tatusova, K. Todorov, B.W. Trawick, D. Vakatov, Y. Wang, M. Ward, W.J. Wilbur, E. Yaschenko, K. Zbicz, Database resources of the national center for Biotechnology information, Nucleic Acids Res. 44 (2016) D7–D19, https://doi.org/10.1093/nar/gkv1290.
[30] R. Agarwala, T. Barrett, J. Beck, D.A. Benson, C. Bollin, E. Bolton, D. Bourexis, J.R. Brister, S.H. Bryant, K. Canese, C. Charowhas, K. Clark, M. DiCuccio, I. Dondoshansky, M. Feolo, K. Funk, L.Y. Geer, V. Gorelenkov, W. Hlavina, M. Hoeppner, B. Holmes, M. Johnson, V. Khotomlianski, A. Kimchi, M. Kimelman, P. Kitts, W. Klimke, S. Krasnov, A. Kuznetsov, M.J. Landrum, D. Landsman, J.M. Lee, D.J. Lipman, Z. Lu, T.L. Madden, T. Madej, A. Marchler-Bauer, I. Karsch-Mizrachi, T. Murphy, R. Orris, J. Ostell, C. O'Sullivan, V. Palanigobu, A.R. Panchenko, L. Phan, K.D. Pruitt, K. Rodarmer, W. Rubinstein, E.W. Sayers, V. Schneider, C.L. Schoch, G.D. Schuler, S.T. Sherry, K. Sirotkin, K. Siyan, D. Slotta, A. Soboleva, V. Soussov, G. Starchenko, T.A. Tatusova, K. Todorov, B.W. Trawick, D. Vakatov, Y. Wang, M. Ward, W.J. Wilbur, E. Yaschenko, K. Zbicz, Database resources of the national center for Biotechnology information, Nucleic Acids Res. 45 (2017) D12–D17, https://doi.org/10.1093/nar/gkw1071.
[31] E. Gasteiger, C. Hoogland, A. Gattiker, S. Duvaud, M.R. Wilkins, R.D. Appel, A. Bairoch, The Proteomics Protocols Handbook, Proteomics Protocols Handbook, 2005, pp. 571–607, https://doi.org/10.1385/1592598900.
[32] R. Gupta, S. Brunak, Prediction of glycosylation across the human proteome and the correlation to protein function, Biocomput 322 (2001) (2002) 310–322, https://doi.org/10.1142/9789812799623_0029.
[33] T.N. Petersen, S. Brunak, G. Von Heijne, H. Nielsen, SignalP 4.0: discriminating signal peptides from transmembrane regions, Nat. Methods 8 (2011) 785–786, https://doi.org/10.1038/nmeth.1701.
[34] A. Marchler-Bauer, M.K. Derbyshire, N.R. Gonzales, S. Lu, F. Chitsaz, L.Y. Geer, R.C. Geer, J. He, M. Gwadz, D.I. Hurwitz, C.J. Lanczycki, F. Lu, G.H. Marchler, J.S. Song, N. Thanki, Z. Wang, R.A. Yamashita, D. Zhang, C. Zheng, S.H. Bryant, CDD: NCBI's conserved domain database, Nucleic Acids Res. 43 (2015) D222–D226, https://doi.org/10.1093/nar/gku1221.
[35] M. Pagni, V. Ioannidis, L. Cerutti, M. Zahn-Zabal, C.V. Jongeneel, J. Hau, O. Martin, D. Kuznetsov, L. Falquet, MyHits: improvements to an interactive resource for analyzing protein sequences, Nucleic Acids Res. 35 (2007) 433–437, https://doi.org/10.1093/nar/gkm352.
[36] M. Biasini, S. Bienert, A. Waterhouse, K. Arnold, G. Studer, T. Schmidt, F. Kiefer, T.G. Cassarino, M. Bertoni, L. Bordoli, T. Schwede, SWISS-MODEL: modelling protein tertiary and quaternary structure using evolutionary information, Nucleic Acids Res. 42 (2014) 252–258, https://doi.org/10.1093/nar/gku340.
[37] F. Sievers, A. Wilm, D. Dineen, T.J. Gibson, K. Karplus, W. Li, R. Lopez, H. McWilliam, M. Remmert, J. Söding, J.D. Thompson, D.G. Higgins, Fast, scalable generation of high-quality protein multiple sequence alignments using Clustal Omega, Mol. Syst. Biol. 7 (2011), https://doi.org/10.1038/msb.2011.75.
[38] W. Li, A. Cowley, M. Uludag, T. Gur, H. McWilliam, S. Squizzato, Y.M. Park, N. Buso, R. Lopez, The EMBL-EBI bioinformatics web and programmatic tools framework, Nucleic Acids Res. 43 (2015) W580–W584, https://doi.org/10.1093/nar/gkv279.
[39] S. Kumar, G. Stecher, K. Tamura, MEGA7: molecular evolutionary genetics analysis version 7.0 for bigger datasets, Mol. Biol. Evol. 33 (2016) 1870–1874, https://doi.org/10.1093/molbev/msw054.
[40] S.A. Bustin, V. Benes, J.A. Garson, J. Hellemans, J. Huggett, M. Kubista, R. Mueller, T. Nolan, M.W. Pfaffl, G.L. Shipley, J. Vandesompele, C.T. Wittwer, The MIQE guidelines: minimum information for publication of quantitative real-time PCR experiments, Clin. Chem. 55 (2009) 611–622, https://doi.org/10.1373/clinchem.2008.112797.
[41] K.J. Livak, T.D. Schmittgen, Analysis of relative gene expression data using real-time quantitative PCR and the 2-ΔΔCT method, Methods 25 (2001) 402–408, https://doi.org/10.1006/meth.2001.1262.
[42] R.L. Stahl, L.F. Liebes, C.M. Farber, R. Silber, A spectrophotometric assay for dehydroascorbate reductase, Anal. Biochem. 131 (1983) 341–344, https://doi.org/10.1016/0003-2697(83)90180-X.
[43] R.B. Silverman, Enzyme Kinetics.pdf, Org. Chem. Enzym. React. (2000) 563–596.
[44] J.-H. Sa, K. Kim, C.-J. Lim, Purification and characterization of glutaredoxin from *Cryptococcus neoformans*, Mol. Cell. 7 (1997) 655–660 http://www.molcells.org/journal/view.html?year=1997&volume=7&number=5&spage=655.
[45] M. Zaffagnini, L. Michelet, V. Massot, P. Trost, S.D. Lemaire, Biochemical characterization of glutaredoxins from Chlamydomonas reinhardtii reveals the unique properties of a chloroplastic CGFS-type glutaredoxin, J. Biol. Chem. 283 (2008) 8868–8876, https://doi.org/10.1074/jbc.M709567200.
[46] P.D. Ray, B.-W. Huang, Y. Tsuji, Reactive oxygen species (ROS) homeostasis and redox regulation in cellular signaling, Cell. Signal. 24 (2012) 981–990, https://doi.org/10.1016/j.cellsig.2012.01.008.Reactive.
[47] S. La Camera, F. L'Haridon, J. Astier, M. Zander, E. Abou-Mansour, G. Page, C. Thurow, D. Wendehenne, C. Gatz, J.P. Métraux, O. Lamotte, The glutaredoxin ATGRXS13 is required to facilitate Botrytis cinerea infection of Arabidopsis thaliana plants, Plant J. 68 (2011) 507–519, https://doi.org/10.1111/j.1365-313X.2011.04706.x.
[48] T. Terada, T. Oshida, M. Nishimura, H. Maeda, T. Hara, S. Hosomi, T. Mizoguchi, T. Nishihara, Study on human erythrocyte thioltransferase: comparative characterization with bovine enzyme and its physiological role under oxidative stress, J. Biochem. 111 (1992) 688–692.
[49] M.R. Fernando, H. Sumimoto, H. Nanri, S. ichiro Kawabata, S. Iwanaga, S. Minakami, Y. Fukumaki, K. Takeshige, Cloning and sequencing of the cDNA encoding human glutaredoxin, Biochim. Biophys. Acta Gene Struct. Expr. 1218 (1994) 229–231, https://doi.org/10.1016/0167-4781(94)90019-1.
[50] N. Foloppe, L. Nilsson, The glutaredoxin -C-P-Y-C- motif: influence of peripheral residues, Structure 12 (2004) 289–300, https://doi.org/10.1016/S0969-2126(04)00021-8.
[51] J.L. Martin, Thioredoxin -a fold for all reasons, Structure 3 (1995) 245–250, https://doi.org/10.1016/S0969-2126(01)00154-X.
[52] C. Berndt, C.H. Lillig, A. Holmgren, Thioredoxins and glutaredoxins as facilitators of protein folding, Biochim. Biophys. Acta Mol. Cell Res. 1783 (2008) 641–650, https://doi.org/10.1016/j.bbamcr.2008.02.003.
[53] E.-M. Hanschmann, J.R. Godoy, C. Berndt, C. Hudemann, C.H. Lillig, Thioredoxins, glutaredoxins, and peroxiredoxins—molecular mechanisms and health significance: from cofactors to antioxidants to redox signaling, Antioxidants Redox Signal. 19 (2013) 1539–1605, https://doi.org/10.1089/ars.2012.4599.
[54] C. Berndt, C.H. Lillig, A. Holmgren, Thiol-based mechanisms of the thioredoxin and glutaredoxin systems: implications for diseases in the cardiovascular system, Am. J. Physiol. Heart Circ. Physiol. 292 (2006) H1227–H1236, https://doi.org/10.1152/ajpheart.01162.2006.
[55] E.S.J. Arnér, A. Holmgren, Physiological functions of thioredoxin and thioredoxin reductase, Eur. J. Biochem. 267 (2000) 6102–6109, https://doi.org/10.1046/j.1432-1327.2000.01701.x.
[56] E.J. Collinson, C.M. Grant, Role of yeast glutaredoxins as glutathione S-transferases, J. Biol. Chem. 278 (2003) 22492–22497, https://doi.org/10.1074/jbc.M301387200.
[57] S.K. Powers, L.L. Ji, A.N. Kavazis, M.J. Jackson, Reactive oxygen species: impact on skeletal muscle, Crit. Rev. Biomed. Eng. 1 (2014) 941–969, https://doi.org/10.1002/cphy.c100054.REACTIVE.
[58] N. Sugino, Reactive oxygen species in ovarian physiology, Reprod. Med. Biol. 4 (2005) 31–44, https://doi.org/10.1111/j.1447-0578.2005.00086.x.
[59] J.X. Wilson, J.X. Wilson, The physiological role of dehydroascorbic acid, FEBS Lett. 527 (2002) 5–9, https://doi.org/10.1016/S0014-5793(02)03167-8.
[60] A.S. Titrant, The structure of partially oxygenated, Hemoglobin 257 (1982) 163–168.
[61] R. Richards, The role of erythrocytes in the inactivation of free radicals, Aust. J. Med. Sci. 17 (1996) 163, https://doi.org/10.1016/S0306-9877(98)90206-7.
[62] V.V. Papov, S.a Gravina, J.J. Mieyal, K. Biemann, The primary structure and properties of thioltransferase (glutaredoxin) from human red blood cells, Protein Sci. 3 (1994) 428–434, https://doi.org/10.1002/pro.5560030307.
[63] H. Minasyan, Erythrocyte and blood antibacterial defense, Eur. J. Microbiol. Immunol. 4 (2014) 138–143, https://doi.org/10.1556/EuJMI.4.2014.2.7.
[64] E. Chantzoura, E. Prinarakis, D. Panagopoulos, G. Mosialos, G. Spyrou, Glutaredoxin-1 regulates TRAF6 activation and the IL-1 receptor/TLR4 signalling, Biochem. Biophys. Res. Commun. 403 (2010) 335–339, https://doi.org/10.1016/j.bbrc.2010.11.029.
[65] C.A. Dinarello, Interleukin-1, cytokine growth factor rev, 8 (1997) 253–265, https://doi.org/10.1016/S1359-6101(97)00023-3.
[66] Y.C. Lu, W.C. Yeh, P.S. Ohashi, LPS/TLR4 signal transduction pathway, Cytokine 42 (2008) 145–151, https://doi.org/10.1016/j.cyto.2008.01.006.
[67] N.L. Reynaert, A. Van Der Vliet, A.S. Guala, T. McGovern, M. Hristova, C. Pantano, N.H. Heintz, J. Heim, Y.-S. Ho, D.E. Matthews, E.F.M. Wouters, Y.M.W. Janssen-Heininger, A. van der Vliet, A.S. Guala, T. McGovern, M. Hristova, C. Pantano, N.H. Heintz, J. Heim, Y.-S. Ho, D.E. Matthews, E.F.M. Wouters, Y.M.W. Janssen-Heininger, Dynamic redox control of NF- kappa B through of inhibitory kappa B kinase $^{\alpha}$, Proc. Natl. Acad. Sci. U. S. A 103 (2006) 13086–13091, https://doi.org/10.1073/pnas.0603290103.
[68] J.M. May, S. Mendiratta, K.E. Hill, R.F. Burk, Reduction of dehydroascorbate to ascorbate by the selenoenzyme thioredoxin reductase, J. Biol. Chem. 272 (1997) 22607–22610, https://doi.org/10.1074/jbc.272.36.22607.
[69] H. Zhou, J. Brock, D. Liu, P.G. Board, A.J. Oakley, Structural insights into the dehydroascorbate reductase activity of human omega-class glutathione transferases, J. Mol. Biol. 420 (2012) 190–203, https://doi.org/10.1016/j.jmb.2012.04.014.
[70] H. Do, I.S. Kim, B.W. Jeon, C.W. Lee, A.K. Park, A.R. Wi, S.C. Shin, H. Park, Y.S. Kim, H.S. Yoon, H.W. Kim, J.H. Lee, Structural understanding of the recycling of oxidized ascorbate by dehydroascorbate reductase (OsDHAR) from Oryza sativa L. japonica, Sci. Rep. 6 (2016) 1–13, https://doi.org/10.1038/srep19498.
[71] J.-A. Bick, F. Aslund, Y. Chen, T. Leustek, Glutaredoxin function for the carboxyl-terminal domain of the plant-type 5'-adenylylsulfate reductase, Proc. Natl. Acad. Sci. Unit. States Am. 95 (1998) 8404–8409, https://doi.org/10.1073/pnas.95.14.8404.
[72] X.H. Gao, M. Zaffagnini, M. Bedhomme, L. Michelet, C. Cassier-Chauvat, P. Decottignies, S.D. Lemaire, Biochemical characterization of glutaredoxins from Chlamydomonas reinhardtii: kinetics and specificity in deglutathionylation reactions, FEBS Lett. 584 (2010) 2242–2248, https://doi.org/10.1016/j.febslet.2010.04.034.
[73] M. Carmack, C.J. Kelley, Synthesis of optically active Cleland's reagent [(-)-1,4-dithio-L-threitol], J. Org. Chem. 33 (1968) 2171–2173, https://doi.org/10.1021/jo01269a123.
[74] A. Holmgren, Thioredoxin catalyzes the reduction of insulin disulfides by dithiothreitol and dihydrolipoamide, J. Biol. Chem. 254 (1979) 9627–9632 10.10.79.

[75] G. Atmaca, Antioxidant effects of sulfur-containing amino acids, Yonsei Med. J. 45 (2004) 776, https://doi.org/10.3349/ymj.2004.45.5.776.
[76] G. Aldini, A. Altomare, G. Baron, G. Vistoli, M. Carini, L. Borsani, F. Sergio, N-Acetylcysteine as an antioxidant and disulphide breaking agent: the reasons why, Free Radic. Res. 52 (2018) 751–762, https://doi.org/10.1080/10715762.2018.1468564.
[77] P. Begas, V. Staudacher, M. Deponte, Systematic re-evaluation of the bis(2-hydroxyethyl)disulfide (HEDS) assay reveals an alternative mechanism and activity of glutaredoxins, Chem. Sci. 6 (2015) 3788–3796, https://doi.org/10.1039/C5SC01051A.
[78] A. Holmgren, [68] Glutaredoxin from Escherichia coli and Calf Thymus, (1985), pp. 525–540, https://doi.org/10.1016/S0076-6879(85)13071-5.
[79] M.M. Gallogly, D.W. Starke, A.K. Leonberg, S.M. English Ospina, J.J. Mieyal, Kinetic and mechanistic characterization and versatile catalytic properties of mammalian glutaredoxin 2: implications for intracellular roles, Biochemistry 47 (2008) 11144–11157, https://doi.org/10.1021/bi800966v.
[80] C. Johansson, C.H. Lillig, A. Holmgren, Human mitochondrial glutaredoxin reduces S-glutathionylated proteins with high affinity accepting electrons from either glutathione or thioredoxin reductase, J. Biol. Chem. 279 (2004) 7537–7543, https://doi.org/10.1074/jbc.M312719200.
[81] M. Weiss, D.F. Steiner, L.H. Philipson, Insulin Biosynthesis, Secretion, Structure, and Structure-Activity Relationships, MDText.com, Inc., 2000 25905258.
[82] D.S. Liyanage, W.K.M. Omeka, G.I. Godahewa, J. Lee, Molecular characterization of thioredoxin-like protein 1 (TXNL1) from big-belly seahorse *Hippocampus abdominalis* in response to immune stimulation, Fish Shellfish Immunol. 75 (2018) 181–189, https://doi.org/10.1016/j.fsi.2018.02.009.